Electrodynamical response of a high-energy photon flux to a gravitational wave

Fang-Yu Li,[1,*] Meng-Xi Tang,[2] Jun Luo,[3] and Yi-Chuan Li[1]
[1]*Department of Physics, Chongqing University, Chongqing 400044, People's Republic of China*
[2]*Department of Physics, Zhongshan University, Guangzhou 510275, People's Republic of China*
[3]*Department of Physics, Huazhong University of Science and Technology, Wuhan 430074, People's Republic of China*
(Received 6 January 2000; published 21 July 2000)

The electrodynamical response of a high-energy photon flux (strong electromagnetic wave) propagating in a static magnetic field to a standing gravitational wave (GW) is studied. The corresponding perturbation solutions and resonant conditions are given. It is found that, for the electromagnetic wave with a frequency ω_e and a standing GW with ω_g, the perturbed electromagnetic fields will contain three new components with frequencies $|\omega_e \pm \omega_g|$ and ω_g, respectively. The resonant response occurs in two cases of $\omega_e = 1/2\omega_g$ (half-frequency resonance) and $\omega_e = \omega_g$ (synchroresonance) only. Then not only first-order axial perturbed power fluxes, which propagate along the same and opposite directions to the background electromagnetic wave, can be generated, but also the radial and tangential perturbed power fluxes can be produced. The latter are perpendicular to the propagating direction of the background electromagnetic wave. This effect might provide a new possibility for the electromagnetic detection of GWs. Moreover, the possible schemes of displaying perturbed effects induced by the high-frequency standing GW at the level of the single photon avalanche and in typical laboratory dimensions are reviewed.

PACS number(s): 04.30.Nk, 04.25.Nx, 04.30.Db

I. INTRODUCTION

In 1916 Einstein published his theory of general relativity, which expected the existence of the gravitational waves (GW's). Nearly 83 years have passed, and yet no gravitational radiation generated in the laboratory has been detected. However, the observation of gravitational radiation from the binary pulsar PSR 1913+16 inspired greatly relevant research, in spite of it providing only indirect evidence for the existence of GW's. Therefore, the direct detection of GW's has become urgently necessary. In 1975 Grishchuk and Sazhin (GS) [1] put forth a scheme of generating high-frequency GW's by a varying electromagnetic (EM) field bound in a toroidal cavity. In the scheme the GWs are focused at the center (focal region) of the toroidal cavity, where they produce a standing GW and could be detected by a detecting cavity put in the focal region. Since this is a scheme in which one hopes to realize both conversions of the EM wave (photons) to GW (gravitons) (i.e., $\gamma \rightarrow g$) and the contrary process ($g \rightarrow \gamma$), and display this effect in a compact structure through achievable limit values of the EM parameters, it caused extensive interest and reviews [2–5].

As pointed out by many authors [2–9], whether from the viewpoint of classical or quantum theories, the conversion rate between the GW's (gravitons) and the EM waves (photons) is extremely low. Thus major difficulties caused by this situation for the GS scheme (including other similar schemes) are [1,5,9]: (1) excessive signal accumulation time $\tau \approx Q/\omega$ for the detecting cavity with high-quality factor Q; (2) the influence of possible leak EM fields from the toroidal cavity (the GW source); (3) giant dimensions and power losses of the whole system (e.g., in order to generate a standing GW with $h = 10^{-33}$, $\lambda_g = 10\,\mathrm{m}$ and detect it, the corresponding signal accumulation time needs 10^5 s, the volumes of the toroidal and detecting cavities are necessarily raised to $2.5 \times 10^4\,\mathrm{m}^3$ and $10\ \mathrm{m}^3$ at least, respectively, and power losses of 10^8 W are required): Although some research [9,10] into overcoming the above difficulties has been done (e.g., the scheme of decreasing signal accumulation time by squeezed quantum states [9], the model of reducing system dimensions by composite cavity [10], *et al.*,), a large gap still exists between the theoretical schemes and reality.

In a recent paper [11], we proposed a new scheme to study the possibility of displaying standing GW by the resonant response of the strong EM wave beam, and given major conclusions in a special case. In this paper we give complete analytic expressions for the perturbation solutions of the EM fields, discuss relative resonant conditions in detail, and derive strict forms of first-order perturbed EM power fluxes. Our results show that if detecting system is not an EM cavity but an EM wave propagating along the symmetrical axis z of the focal region of the toroidal cavity, where a static magnetic field pointing along the z axis is distributed in the focal region, then under the special resonant conditions, it is possible to provide a new way of simultaneously narrowing such gaps. Namely, for the resonant states, the key parameters are not the total net increasing quantities of the EM energy (photon number) but the change of the physical behavior of the EM fields (photons) caused by the GW. In other words, even if the net increasing quantities approach zero, the perturbed effect on behavior is obviously different from that of the background EM fields and can be generated in the local regions. This property may be very useful to display very weak signals of the GWs.

*Email address: fangyuli@public.cta.cq.cn

II. ELECTRODYNAMICAL RESPONSE OF A STRONG ELECTROMAGNETIC WAVE PROPAGATING IN A STATIC MAGNETIC FIELD TO A STANDING GRAVITATIONAL WAVE

In order to make the whole system have an acceptable size, we study the electrodynamical response to the high-frequency standing GW with $\nu=10^8-10^9$ Hz. For the EM detection of the high-frequency GW's, we can adopt the synchronous gauge reference used in Refs. [1,12] (this has been reviewed in Refs. [1,12,13] and we shall not repeat it here). In the focal region of the toroidal cavity, the form of the standing GW in the synchronous gauge reference (and using standard cylindrical polar coordinates expressions) is [1,10]

$$h_{rr}=-A\frac{J_1(k_g r)}{k_g r}\cos(\omega_g t+\delta),$$

$$h_{\phi\phi}=-Ar^2\left[J_0(k_g r)-\frac{J_1(k_g r)}{k_g r}\right]\cos(\omega_g t+\delta),$$

$$h_{zz}=AJ_0(k_g r)\cos(\omega_g t+\delta), \tag{1}$$

where A is the amplitude of the standing GW, J_0, J_1 are Bessel functions, ω_g, k_g are the angular frequency and the wave vector of the GW, respectively, δ is a retarded phase factor. Letting $(x^0,x^1,x^2,x^3)=(ct,r,\phi,z)$, from Eq. (1), we get

$$g_{00}=1,\quad g_{11}=g_{rr}=-1+h_{rr},\quad g_{22}=g_{\phi\phi}=-r^2+h_{\phi\phi},$$

$$g_{33}=g_{zz}=-1+h_{zz},$$

$$g^{00}=1,\quad g^{11}=g^{rr}=-1-h_{rr},$$

$$g^{22}=g^{\phi\phi}=-\frac{1}{r^2}\left(1+\frac{h_{\phi\phi}}{r^2}\right),$$

$$g^{33}=g^{zz}=-1-h_{zz}. \tag{2}$$

The electrodynamical response to the GW can be described by the Maxwell equations in curved space-time (we use MKS units), i.e.,

$$\frac{1}{\sqrt{-g}}\frac{\partial}{\partial x^\nu}(\sqrt{-g}g^{\mu\alpha}g^{\nu\beta}F_{\alpha\beta})=\mu_0 j^\mu, \tag{3}$$

$$F_{[\mu\nu,\alpha]}=0, \tag{4}$$

where $F_{\mu\nu}$, j^μ indicate the EM field tensor and four-dimensional electric current density, respectively. For the electrodynamical response in the vacuum, because it has neither the real four-dimensional electric current nor the equivalent electric current caused by the energy dissipation, such as Ohmic losses in the cavity walls or the dielectric losses (e.g., see, Ref. [1]), so that $j^\mu=0$ in Eq. (3). For the effect of the weak GW field, $F_{\mu\nu}$ can always be written as $F_{\mu\nu}=F^{(0)}_{\mu\nu}+F^{(1)}_{\mu\nu}$, and $|F^{(1)}_{\mu\nu}|\ll|F^{(0)}_{\mu\nu}|$ for the nonvanishing $F^{(0)}_{\mu\nu}$ and $F^{(1)}_{\mu\nu}$. Here $F^{(0)}_{\mu\nu}$ represents the background field, $F^{(1)}_{\mu\nu}$ is the first-order perturbation to $F^{(0)}_{\mu\nu}$ in the presence of the GW.

Unlike the cavity electrodynamical response to the GW [1,12], our detecting system is an EM wave propagating in a static magnetic field distributed in the focal region, i.e.,

$$B^{(0)}=B^{(0)}_z=\text{const},\quad E^{(0)}_x=a\cos(k_e z-\omega_e t),$$

$$B^{(0)}_y=\frac{a}{c}\cos(k_e z-\omega_e t).$$

In the cylindrical polar coordinates they can be written as

$$B^{(0)}=B^{(0)}_z=\text{const}, \tag{5}$$

$$E^{(0)}_r=a\cos\phi\cos(k_e z-\omega_e t),$$

$$E^{(0)}_\phi=-a\sin\phi\cos(k_e z-\omega_e t),$$

$$B^{(0)}_r=\frac{a}{c}\sin\phi\cos(k_e z-\omega_e t),$$

$$B^{(0)}_\phi=\frac{a}{c}\cos\phi\cos(k_e z-\omega_e t). \tag{6}$$

For simplifying calculations, we give complete perturbation solutions by two steps.

A. The first-order perturbation to the static magnetic field

First, we assume that the detecting EM field is only a static magnetic field, Eq. (5), then the components of $F_{\mu\nu}$ in the cylindrical polar coordinates are

$$F_{01}=F^{(1)}_{01}=\frac{E^{(1)}_r}{c},\quad F_{02}=F^{(1)}_{02}=\frac{rE^{(1)}_\phi}{c},\quad F_{03}=F^{(1)}_{03}=\frac{E^{(1)}_z}{c},$$

$$F_{12}=F^{(0)}_{12}+F^{(1)}_{12}=-r(B^{(0)}_z+B^{(1)}_z),\quad F_{13}=F^{(1)}_{13}=B^{(1)}_\phi,$$

$$F_{23}=F^{(1)}_{23}=-rB^{(1)}_r. \tag{7}$$

Introducing Eqs. (1), (2), and (7), into Eqs. (3) and (4), neglecting high-order infinite small quantities, we obtain following first-order perturbation equations:

$$(\Box E^{(1)})_\phi=E^{(1)}_{\phi,rr}+\frac{1}{r}E^{(1)}_{\phi,r}+\frac{1}{r^2}E^{(1)}_{\phi,\phi\phi}+E^{(1)}_{\phi,zz}-\frac{1}{r^2}E^{(1)}_\phi+\frac{2}{r^2}E^{(1)}_{r,\phi}-\frac{1}{c^2}E^{(1)}_{\phi,tt}$$
$$=-AcB^{(0)}_z k_g^2 J_1(k_g r)\sin(\omega_g t+\delta), \tag{8}$$

$$(\Box B^{(1)})_z=B^{(1)}_{z,rr}+\frac{1}{r}B^{(1)}_{z,r}+\frac{1}{r^2}B^{(1)}_{z,\phi\phi}+B^{(1)}_{z,zz}-\frac{1}{c^2}B^{(1)}_{z,tt}$$
$$=-AB^{(0)}_z k_g^2 J_0(k_g r)\cos(\omega_g t+\delta), \tag{9}$$

$$(\Box E^{(1)})_r=(\Box E^{(1)})_z=0,(\Box B^{(1)})_r=(\Box B^{(1)})_\phi=0, \tag{10}$$

where $\Box$ expresses the d'Alembertian in the cylindrical polar coordinates, and the commas denote partial derivatives. Solving Eqs. (8)–(10), and considering cylindrical symmetry of the fields in the focal region, we get following perturbation solutions:

$$E_{\phi}^{(1)}=\frac{1}{2}AcB_z^{(0)}k_g r J_0(k_g r)\sin(\omega_g t+\delta),$$

$$B_z^{(1)}=AB_z^{(0)}\left[J_0(k_g r)-\frac{1}{2}k_g r J_1(k_g r)\right]\cos(\omega_g t+\delta),$$

$$E_r^{(1)}=E_z^{(1)}=B_r^{(1)}=B_{\phi}^{(1)}=0. \tag{11}$$

B. The first-order perturbation to the electromagnetic wave

Second, we assume that detecting EM field is only the EM wave, Eq. (6), then the components of $F_{\mu\nu}$ are

$$F_{01}=F_{01}^{(0)}+\tilde{F}_{01}^{(1)}=\frac{E_r^{(0)}+\tilde{E}_r^{(1)}}{c},$$

$$F_{02}=F_{02}^{(0)}+\tilde{F}_{02}^{(1)}=\frac{r(E_{\phi}^{(0)}+\tilde{E}_{\phi}^{(1)})}{c},$$

$$F_{03}=\tilde{F}_{03}^{(1)}=\frac{\tilde{E}_z^{(1)}}{c},\quad F_{12}=\tilde{F}_{12}^{(1)}=-r\tilde{B}_z^{(1)},$$

$$F_{13}=F_{13}^{(0)}+\tilde{F}_{13}^{(1)}=B_{\phi}^{(0)}+\tilde{B}_{\phi}^{(1)},$$

$$F_{23}=F_{23}^{(0)}+\tilde{F}_{23}^{(1)}=-r(B_r^{(0)}+\tilde{B}_r^{(1)}). \tag{12}$$

where $\tilde{F}_{\mu\nu}^{(1)}$ represents the first-order perturbation produced by the direct interaction of the standing GW with the background EM wave. Introducing Eqs. (1), (2), and (12) into Eqs. (3) and (4), neglecting high-order infinite small quantities, in the same way, one finds first-order perturbation equations as follows:

$$\begin{aligned}(\Box\tilde{E}^{(1)})_r&=\tilde{E}_{r,rr}^{(1)}+\frac{1}{r}\tilde{E}_{r,r}^{(1)}+\frac{1}{r^2}\tilde{E}_{r,\phi\phi}^{(1)}+\tilde{E}_{r,zz}^{(1)}-\frac{1}{r^2}\tilde{E}_r^{(1)}-\frac{2}{r^2}\tilde{E}_{\phi,\phi}^{(1)}-\frac{1}{c^2}\tilde{E}_{r,tt}^{(1)}\\&=\frac{1}{2}Aac\left[(k_e^2+k_ek_g)J_0(k_gr)+\frac{1}{r}(k_g+k_e)J_1(k_gr)+\frac{1}{r^2}J_0(k_gr)-\frac{1}{k_er^3}J_1(k_gr)\right]\cos\phi\cos[(\omega_g+\omega_e)t-k_ez+\delta]\\&\quad+\frac{1}{2}Aac\left[(k_e^2-k_ek_g)J_0(k_gr)+\frac{1}{r}(k_g-k_e)J_1(k_gr)+\frac{1}{r^2}J_0(k_gr)-\frac{1}{k_er^3}J_1(k_gr)\right]\\&\quad\times\cos\phi\cos[(\omega_g-\omega_e)t+k_ez+\delta],\end{aligned} \tag{13}$$

$$\begin{aligned}(\Box\tilde{E}^{(1)})_{\phi}&=\tilde{E}_{\phi,rr}^{(1)}+\frac{1}{r}\tilde{E}_{\phi,r}^{(1)}+\frac{1}{r^2}\tilde{E}_{\phi,\phi\phi}^{(1)}+\tilde{E}_{\phi,zz}^{(1)}-\frac{1}{r^2}\tilde{E}_{\phi}^{(1)}+\frac{2}{r^2}\tilde{E}_{r,\phi}^{(1)}-\frac{1}{c^2}\tilde{E}_{\phi,tt}^{(1)}\\&=\frac{1}{2}Aac\left[-(k_e+k_g)^2J_0(k_gr)+\frac{1}{r}(k_g+k_e)J_1(k_gr)\right]\sin\phi\cos[(\omega_g+\omega_e)t-k_ez+\delta]+\frac{1}{2}Aac\Big[-(k_e\\&\quad-k_g)^2J_0(k_gr)+\frac{1}{r}(k_g-k_e)J_1(k_gr)\Big]\sin\phi\cos[(\omega_g-\omega_e)t+k_ez+\delta],\end{aligned} \tag{14}$$

$$\begin{aligned}(\Box\tilde{E}^{(1)})_z&=\tilde{E}_{z,rr}^{(1)}+\frac{1}{r}\tilde{E}_{z,r}^{(1)}+\frac{1}{r^2}\tilde{E}_{z,\phi\phi}^{(1)}+\tilde{E}_{z,zz}^{(1)}-\frac{1}{c^2}\tilde{E}_{z,tt}^{(1)}\\&=\frac{1}{2}Aac\left[-(k_g^2+k_ek_g)J_1(k_gr)-\frac{2k_e}{r}J_0(k_gr)+\frac{4k_e}{k_gr^2}J_1(k_gr)\right]\cos\phi\sin[(\omega_g+\omega_e)t-k_ez+\delta]\\&\quad+\frac{1}{2}Aac\left[-(k_g^2-k_ek_g)J_1(k_gr)+\frac{2k_e}{r}J_0(k_gr)-\frac{4k_e}{k_gr^2}J_1(k_gr)\right]\cos\phi\sin[(\omega_g-\omega_e)t+k_ez+\delta].\end{aligned} \tag{15}$$

It can be shown that the first-order perturbed magnetic field satisfies the similar equations. Eqs. (13)–(15) consist of group of the inhomogeneous hyperbolic-type equations, and the right side of the equations group contains the product of Bessel functions with factors $1/r$, $1/r^2$, and $1/r^3$, solving directly these equations is very difficult. Fortunately, using series method, after a length calculation, we get corresponding solutions for Eqs. (13)–(15) together with Eq. (4) as follows:

$$\tilde{E}_r^{(1)}=A_1(r)\cos\phi\cos[(\omega_g+\omega_e)t-k_ez+\delta]+A_2(r)\cos\phi\cos[(\omega_g-\omega_e)t+k_ez+\delta],$$

$$\tilde{E}_\phi^{(1)}=B_1(r)\sin\phi\cos[(\omega_g+\omega_e)t-k_ez+\delta]+B_2(r)\sin\phi\cos[(\omega_g-\omega_e)t+k_ez+\delta],$$

$$\tilde{E}_z^{(1)}=C_1(r)\cos\phi\sin[(\omega_g+\omega_e)t-k_ez+\delta]+C_2(r)\cos\phi\sin[(\omega_g-\omega_e)t+k_ez+\delta],$$

$$\tilde{B}_r^{(1)}=\frac{1}{c(k_g+k_e)}\left[k_eB_1(r)+\frac{C_1(r)}{r}\right]\sin\phi\{\cos(k_ez-\delta)-\cos[(\omega_g+\omega_e)t-k_ez+\delta]\}-\frac{1}{c(k_g-k_e)}$$
$$\times\left[k_eB_2(r)-\frac{C_2(r)}{r}\right]\sin\phi\{\cos(k_ez+\delta)-\cos[(\omega_g-\omega_e)t+k_ez+\delta]\},$$

$$\tilde{B}_\phi^{(1)}=\frac{-1}{c(k_g+k_e)}\left[k_eA_1(r)-\frac{dB_1(r)}{dr}\right]\cos\phi\{\cos(k_ez-\delta)-\cos[(\omega_g+\omega_e)t-k_ez+\delta]\}+\frac{1}{c(k_g-k_e)}$$
$$\times\left[k_eA_2(r)+\frac{dB_2(r)}{dr}\right]\cos\phi\{\cos(k_ez+\delta)-\cos[(\omega_g-\omega_e)t+k_ez+\delta]\},$$

$$\tilde{B}_z^{(1)}=\frac{-1}{c(k_g+k_e)}\left[\frac{A_1(r)+B_1(r)}{r}+\frac{dB_1(r)}{dr}\right]\sin\phi\{\sin(k_ez-\delta)-\sin[(\omega_g+\omega_e)t-k_ez+\delta]\}+\frac{1}{c(k_g-k_e)}$$
$$\times\left[\frac{A_2(r)+B_2(r)}{r}+\frac{dB_2(r)}{dr}\right]\sin\phi\{\sin(k_ez+\delta)-\sin[(\omega_g-\omega_e)t+k_ez+\delta]\},\tag{16}$$

where A_1, A_2, B_1, B_2, C_1, and C_2 are functions of r, k_e, and k_g, their concrete forms are presented in Appendix [see, Eqs. (A1)–(A8)].

Obviously, when both the static magnetic field and the background EM wave are simultaneously present, the complete perturbation solutions should be Eq. (11) plus Eq. (16), i.e., $\tilde{E}_r^{(1)}$, $E_\phi^{(1)}+\tilde{E}_\phi^{(1)}$, $\tilde{E}_z^{(1)}$, $\tilde{B}_r^{(1)}$, $\tilde{B}_\phi^{(1)}$, and $B_z^{(1)}+\tilde{B}_z^{(1)}$. In passing, we note that the above forms of the analytic solutions are quite complicated, but as we show under the resonant conditions (especially the synchroresonance), the first-order perturbed EM power fluxes will be reduced to the simpler forms [e.g., see, Eqs. (24) and (26)].

C. The electrodynamical response to the standing gravitational wave

The expression of the energy-momentum tensor of the EM fields in the GW field is given by

$$T^{\mu\nu}=\frac{1}{\mu_0}\left(-F^{\mu}{}_{\alpha}F^{\nu\alpha}+\frac{1}{4}g^{\mu\nu}F_{\alpha\beta}F^{\alpha\beta}\right).\tag{17}$$

Due to $F^{\mu\nu}=\overset{(0)}{F}{}^{\mu\nu}+\overset{(1)}{F}{}^{\mu\nu}$ and $|F_{\mu\nu}^{(1)}|\ll|F_{\mu\nu}^{(0)}|$ for the nonvanishing $F_{\mu\nu}^{(0)}$ and $F_{\mu\nu}^{(1)}$, $T^{\mu\nu}$ can be disintegrated into

$$T^{\mu\nu}=\overset{(0)}{T}{}^{\mu\nu}+\overset{(1)}{T}{}^{\mu\nu}+\overset{(2)}{T}{}^{\mu\nu},\tag{18}$$

where $\overset{(0)}{T}{}^{\mu\nu}$ is the energy-momentum tensor of the background EM fields, and $\overset{(1)}{T}{}^{\mu\nu}$ and $\overset{(2)}{T}{}^{\mu\nu}$ represent first- and second-order perturbations to $\overset{(0)}{T}{}^{\mu\nu}$ in the presence of the GW respectively. For the nonvanishing $\overset{(0)}{T}{}^{\mu\nu}$, $\overset{(1)}{T}{}^{\mu\nu}$, and $\overset{(2)}{T}{}^{\mu\nu}$, we have

$$|\overset{(0)}{T}{}^{\mu\nu}|\gg|\overset{(1)}{T}{}^{\mu\nu}|\gg|\overset{(2)}{T}{}^{\mu\nu}|\approx O(h^2).\tag{19}$$

Therefore, for the effect of the GW, we are interested in $\overset{(1)}{T}{}^{\mu\nu}$ but not in $\overset{(0)}{T}{}^{\mu\nu}$ and $\overset{(2)}{T}{}^{\mu\nu}$. From Eqs. (5)–(7), (11), (12), (16), and (17), we obtain

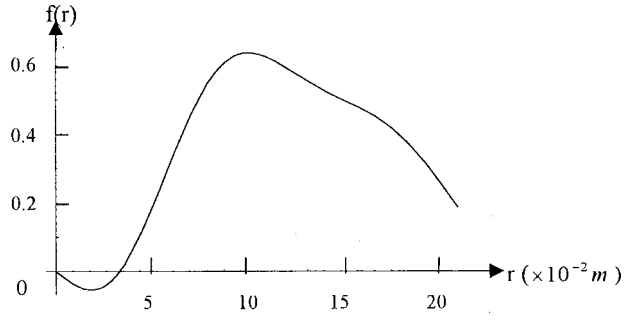

FIG. 1. Rating curve between the function $f(r)$, Eq. (25), and the radial coordinate r, here $\lambda_e=2\lambda_g=0.2$ m. In fact, when the summation in Eq. (25) reached $p=23$, $f(r)$ already approached a stable value for any definite r and k_e.

$$\overset{(1)}{T}{}^{00}=\varepsilon_0\left[E_r^{(0)}\tilde{E}_r^{(1)}+E_\phi^{(0)}(E_\phi^{(1)}+\tilde{E}_\phi^{(1)})+\frac{1}{2}h_{rr}(E_r^{(0)})^2+\frac{1}{2}\frac{h_{\phi\phi}}{r^2}(E_\phi^{(0)})^2\right]+\frac{1}{\mu_0}\left[B_r^{(0)}\tilde{B}_r^{(1)}+B_\phi^{(0)}\tilde{B}_\phi^{(1)}+B_z^{(0)}(B_z^{(1)}+\tilde{B}_z^{(1)})\right.$$
$$\left.+\frac{1}{2}\left(h_{zz}+\frac{h_{\phi\phi}}{r^2}\right)(B_r^{(0)})^2+\frac{1}{2}(h_{rr}+h_{zz})(B_\phi^{(0)})^2+\frac{1}{2}\left(h_{rr}+\frac{h_{\phi\phi}}{r^2}\right)(B_z^{(0)})^2\right], \tag{20}$$

$$\overset{(1)}{S}{}^r=c\overset{(1)}{T}{}^{01}=\frac{1}{\mu_0}(E_\phi^{(0)}B_z^{(1)}+E_\phi^{(0)}\tilde{B}_z^{(1)}-\tilde{E}_z^{(1)}B_\phi^{(0)}+E_\phi^{(1)}B_z^{(0)}+\tilde{E}_\phi^{(1)}B_z^{(0)}), \tag{21}$$

$$\overset{(1)}{S}{}^\phi=c\overset{(1)}{T}{}^{02}=\frac{1}{\mu_0}(\tilde{E}_z^{(1)}B_r^{(0)}-E_r^{(0)}B_z^{(1)}-E_r^{(0)}\tilde{B}_z^{(1)}-\tilde{E}_r^{(1)}B_z^{(0)}), \tag{22}$$

$$\overset{(1)}{S}{}^z=c\overset{(1)}{T}{}^{03}=\frac{1}{\mu_0}(E_r^{(0)}\tilde{B}_\phi^{(1)}+\tilde{E}_r^{(1)}B_\phi^{(0)}-E_\phi^{(0)}\tilde{B}_r^{(1)}-E_\phi^{(1)}B_r^{(0)}-\tilde{E}_\phi^{(1)}B_r^{(0)}), \tag{23}$$

where $\overset{(1)}{T}{}^{00}$ is the first-order perturbed energy density of the EM fields, while $\overset{(1)}{S}{}^r$, $\overset{(1)}{S}{}^\phi$, and $\overset{(1)}{S}{}^z$ represent first-order radial, tangential, and axial perturbed power fluxes, respectively. It must be pointed out that for the high-frequency perturbed power flux, only nonvanishing average terms of it with respect to time have observable effect. It is easily seen from Eqs. (11), (16), and (21)–(23), that the average values of the perturbed power fluxes, Eqs. (21)–(23), vanish in whole frequency ranges of $\omega_e\neq\omega_g$ and $\omega_e\neq 1/2\omega_g$. In other words, only under the condition of $\omega_e=1/2\omega_g$ (half-frequency resonance) or $\omega_e=\omega_g$ (synchrorenance), do $\overset{(1)}{S}{}^r$, $\overset{(1)}{S}{}^\phi$, and $\overset{(1)}{S}{}^z$ (including $\overset{(1)}{T}{}^{00}$) have nonvanishing average values with respect to time. In the following we study only the tangential perturbed power flux $\langle\overset{(1)}{S}{}^\phi\rangle$, here the angular brackets denote the average value with respect to time. Introducing Eqs. (5), (6), (11), (16), and (A1)–(A8) into Eq. (22), and setting $\delta=\pi$ (it is always possible), we have

$$\langle\overset{(1)}{S}{}^\phi\rangle_{\omega_e=1/2\omega_g}=\frac{1}{\mu_0}\langle\tilde{E}_z^{(1)}B_r^{(0)}-E_r^{(0)}\tilde{B}_z^{(1)}\rangle_{\omega_e=1/2\omega_g}=\frac{Aa^2}{8\mu_0 c}f(r)\sin 2\phi\sin(k_g z), \tag{24}$$

where

$$f(r)=\sum_{p=0}^{\infty}(-1)^{p+1}\left\{\left[\frac{2p^2+8p+7}{[(2p+4)^2-4](p+1)!(p+2)!}-\frac{2p+6}{[(2p+3)^2-1]p!(p+2)!}\right]k_e^{2p+3}r^{2p+3}+\frac{k_e^{2p+1}r^{2p+1}}{4(p+1)!(p+2)!}\right\}. \tag{25}$$

Figure 1 gives the rating curve between the function $f(r)$ and the radial coordinate r, and relative parameters are chosen as $\lambda_e=2\lambda_g=0.2\,\mathrm{m}$. Figures 2 and 3 give distributions of $\langle\overset{(1)}{S}{}^\phi\rangle_{\omega_e=1/2\omega_g}$ at the planes $z=\pm\lambda_g/4$, respectively.

Using Eqs. (5), (6), (11), (16), and (22), in the same way, one finds

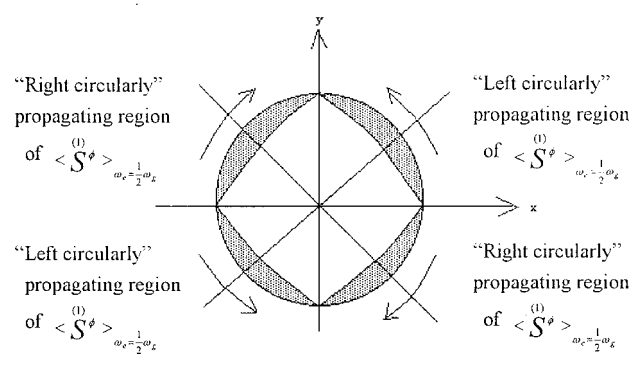

FIG. 2. Distribution of $\langle\overset{(1)}{S}{}^\phi\rangle_{\omega_e=1/2\omega_g}$ at the plane $z=\lambda_g/4$. It has maximum at $\phi=\pi/4$, $3\pi/4$, $5\pi/4$, and $7\pi/4$, while it vanishes at $\phi=0$, $\pi/2$, π, and $3\pi/2$, here $r=0.2$ m.

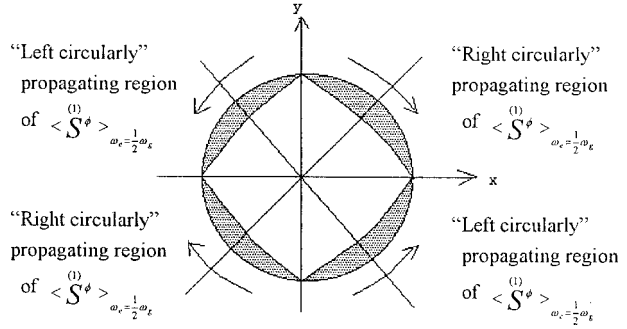

FIG. 3. Distribution of $\langle\overset{(1)}{S}{}^\phi\rangle_{\omega_e=1/2\omega_g}$ at the plane $z=-\lambda_g/4$. It has maximum at $\phi=\pi/4$, $3\pi/4$, $5\pi/4$, and $7\pi/4$, while it vanishes at $\phi=0$, $\pi/2$, π, and $3\pi/2$, but the directions are contrary to that at the plane $z=\lambda_g/4$, here $r=0.2$ m.

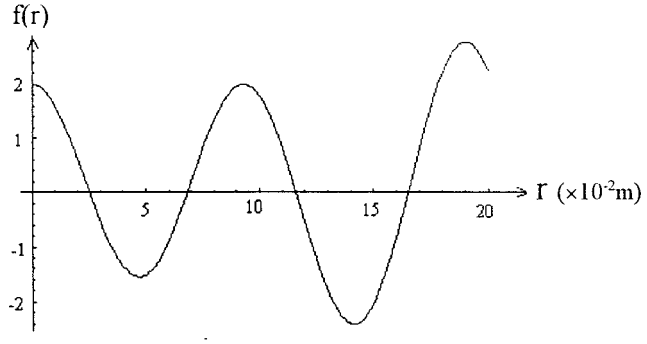

FIG. 4. Rating curve between the radial coordinates r and the function $f(r)=2J_0(k_gr)-k_grJ_1(k_gr)$, here $\lambda_e=\lambda_g=0.1$ m.

$$\langle S^{(1)\phi}\rangle_{\omega_e=\omega_g}=-\frac{1}{\mu_0}\langle E_r^{(0)}B_z^{(1)}\rangle_{\omega_e=\omega_g}$$
$$=\frac{AaB_z^{(0)}}{4\mu_0}[2J_0(k_gr)$$
$$-k_grJ_1(k_gr)]\cos\phi\cos(k_gz). \qquad (26)$$

We see that $\langle S^{(1)\phi}\rangle_{\omega_e=\omega_g}$ contains no contribution of $\tilde{F}^{(1)}_{\mu\nu}$.

Figure 4 gives the rating curve between the radial coordinate r and the function $f(r)=2J_0(k_gr)-k_grJ_1(k_gr)$, relative parameters are chosen as $\lambda_e=\lambda_g=0.1$ m. Figures 5 and 6 give distributions of $\langle S^{(1)\phi}\rangle_{\omega_e=\omega_g}$ at the planes $z=0$ and $z=\lambda_e/2$, respectively.

Figures 1–6 and Eqs. (24)–(26) indicate that $\langle S^{(1)\phi}\rangle$ is often a function of the space coordinates r, ϕ, z, and there are corresponding ''equivalent emission sources.'' Therefore, $S^{(1)\phi}$ is essentially a power flux (photon flux) fluctuation superimposed on the background EM fields. From the viewpoint of quantum theory, the above-mentioned properties express actually the change of the physical behavior of the photons (e.g., propagating directions and distributions in the local regions). This change is caused by the scattering of the gravitons to a large amount of the photons. If there are no net increasing photons in the first-order perturbation, then this process should be the elastic scattering of the gravitons to the photons, not their resonant conversion, the latter corresponds only to the second-order perturbation to the energy-momentum tensor of the background EM fields at classical level.

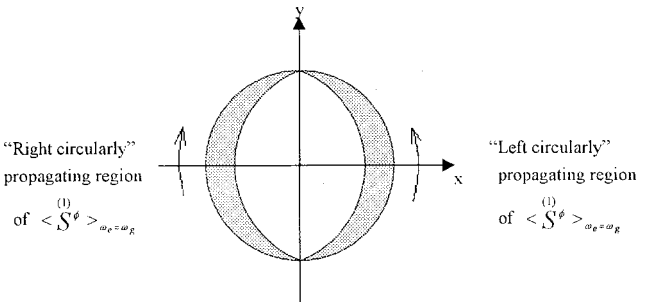

FIG. 5. Distribution of $\langle S^{(1)\phi}\rangle_{\omega_e=\omega_g}$ at the plane $z=0$. It has maximum at $\phi=0$, π, while it vanishes at $\phi=\pm\pi/2$, here $r=\lambda_e=\lambda_g=0.1$ m.

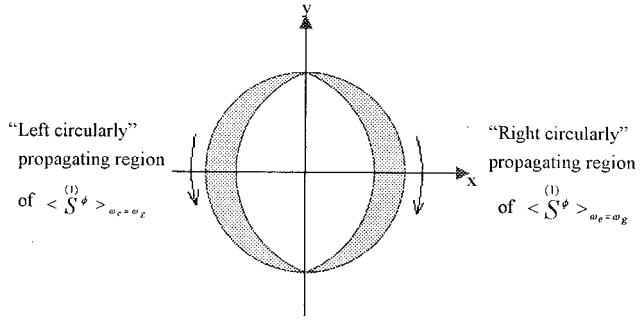

FIG. 6. Distribution of $\langle S^{(1)\phi}\rangle_{\omega_e=\omega_g}$ at the plane $z=\lambda_g/2$. It has maximum at $\phi=0$, π, while it vanishes at $\phi=\pm\pi/2$, but the directions are contrary to that at the plane $z=0$, here $r=\lambda_e=\lambda_g=0.1$ m.

Integration of Eq. (26) over the plane $\phi=0$ ($0\leqslant r\leqslant R_c$, $-\lambda_g/4\leqslant z\leqslant\lambda_g/4$) gives the total power flux passing through the plane as follows:

$$\langle u^{(1)\phi}\rangle_{\omega_e=\omega_g,\phi=0}=\int_0^{R_c}\int_{-\lambda_g/4}^{\lambda_g/4}\langle S^{(1)\phi}\rangle_{\omega_e=\omega_g,\phi=0}drdz$$
$$=\frac{AB_z^{(0)}a}{2\mu_0k_g}\int_0^{R_c}[2J_0(k_gr)-k_grJ_1(k_gr)]dr. \qquad (27)$$

Figure 7 gives the rating curve between the function $F(R_c)=\int_0^{R_c}[2J_0(k_gr)-k_grJ_1(k_gr)]dr$ and R_c, and the relative parameters are chosen as $\lambda_e=\lambda_g=0.1$ m. We see that the second maximum of the resonance response occurs in the case of $R_c\approx1.2\lambda_g=0.12$ m and then $F(R_c)\approx0.05$ m. This means that the effective perturbed power flux can be concentrated on the region with magnitude of a wavelength λ_g near the axis.

According to Eqs. (5)–(7), (11), (16), (17), (20), (21), (23), and (A1)–(A8), in the same way, one can give the

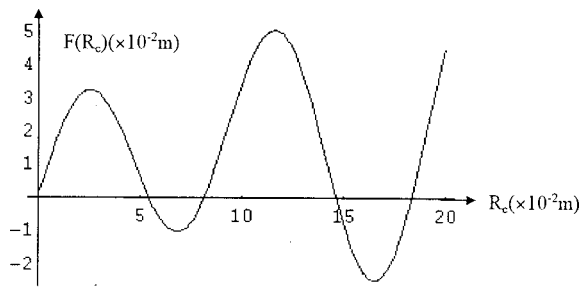

FIG. 7. Rating curve between the function $F(R_c)=\int_0^{R_c}[2J_0(k_gr)-k_grJ_1(k_gr)]dr$ and R_c. The relative parameters are chosen as $\lambda_e=\lambda_g=0.1$ m.

average values: $\langle \overset{(1)}{T^{00}} \rangle_{\omega_e=1/2\omega_g}$, $\langle \overset{(1)}{T^{00}} \rangle_{\omega_e=\omega_g}$, $\langle \overset{(1)}{S^r} \rangle_{\omega_e=1/2\omega_g}$, $\langle \overset{(1)}{S^r} \rangle_{\omega_e=\omega_g}$, $\langle \overset{(1)}{S^z} \rangle_{\omega_e=1/2\omega_g}$, and $\langle \overset{(1)}{S^z} \rangle_{\omega_e=\omega_g}$. One can also show that even the total net increasing quantities of the EM energy (photon number) approach zero in the whole resonant region, i.e., $\int \langle \overset{(1)}{T^{00}} \rangle_{\omega_e=\omega_g} d^3x \to 0$ or $\int \langle \overset{(1)}{T^{00}} \rangle_{\omega_e=1/2\omega_g} d^3x \to 0$, the perturbed effect (i.e., nonvanishing first-order perturbed power flux) can be generated in the local regions. Its behavior obviously is different from that of the background EM fields.

III. NUMERICAL ESTIMATIONS

For the standing GW distributed in the focal region of the toroidal cavity, the amplitude magnitude is given by [1]

$$A \approx \frac{GW_e}{c^4 R} \approx \frac{Gw_e V}{c^4 R}, \tag{28}$$

where W_e and w_e are the total energy and the average energy density of the EM field stored in the toroidal cavity, respectively, V is the volume of the cavity, and R is its inner radius. In order to reduce the length of this paper, we consider only $\langle \overset{(1)}{u^{\phi}} \rangle_{\omega_e=\omega_g}$. Then the corresponding tangential perturbed photon flux of $\langle \overset{(1)}{u^{\phi}} \rangle_{\omega_e=\omega_g}$ can be written as

$$n = \frac{\langle \overset{(1)}{u^{\phi}} \rangle_{\omega_e=\omega_g}}{\hbar \omega_e}, \tag{29}$$

where $\hbar$ is Planck constant. Therefore, the perturbed photon number caused by $\langle \overset{(1)}{u^{\phi}} \rangle_{\omega_e=\omega_g}$ in the duration Δt is

$$N = n\Delta t = \frac{AB_z^{(0)} a \Delta t}{2\mu_0 k_g \hbar \omega_e} \int_0^{R_c} [2J_0(k_g r) - k_g r J_1(k_g r)] dr. \tag{30}$$

For finding a reasonable scheme, we choose following parameters: (1) $a = 3\times 10^5\ \mathrm{V\,m^{-1}}$, $a/c = 10^{-3}\ \mathrm{T}$, the amplitude of the background EM wave. If the cross section of the background EM wave is limited in the region of radius $R_c = \lambda_e = \lambda_g = 0.1\ \mathrm{m}$ (namely, the EM wave beam), then the corresponding power is about $10^6\ \mathrm{W}$. This is equivalent to photon flux $n^{(0)}$ of $10^{30}\ \mathrm{s^{-1}}$ roughly for the background EM wave of $\lambda_e = 0.1\ \mathrm{m}$. Modern klystrons or free-electron lasers can, in principle, generate such a power [6]. Strictly speaking, the background EM wave expressed by Eq. (6) is only an ideal form, because any realized EM wave beams and static magnetic fields need corresponding boundary conditions, and it is necessary to consider the energy contribution at the boundary. However, the Gauss light (EM wave) beam [14] is just one of the realized EM wave beams, and it is always possible to construct an abrupt boundary with Gaussian distribution (generating an approximate uniform static magnetic field in a finite region is also always possible). Although this wave beam is different from the background EM wave, some features (such as the propagating directions, distributions, and strengths) of the first-order perturbed power fluxes produced by the standing GW are quite similar, and the energy contribution to the perturbed power fluxes at the boundary is negligible. We will give further argument to these questions in a later paper. (2) $B_z^{(0)} = 30\ \mathrm{T}$, the strength of the background static magnetic field (this is achievable strength of a stationary magnetic field in present experiments, while a pulse magnetic field may reach up to $10^2 - 10^3\ \mathrm{T}$ [15]). Notice that although this is a very strong field, one requires only that this static field be localized in the focal region with $R_c = 0.1\ \mathrm{m}$ ($R_c \ll R$) near the axis. (3) $R_c = 0.1\ \mathrm{m}$, the radius of the focal region; $R = 3\ \mathrm{m}$, the inner radius of the toroidal cavity. (4) $Q = 10^{13}$, $w_e = 10^9\ \mathrm{J\,m^{-3}}$, the typical parameters used in Refs. [1], [2], [9] and [16]. (In fact, the Q value of a superconducting microwave cavity may reach up to $10^{15} - 10^{16}$ [9,17]). (5) The power losses of the cavity can be estimated as $P \approx W_e \omega_e / Q$ [18].

TABLE I. The perturbed photon number N and corresponding relevant parameters.

$\langle \overset{(1)}{u^{\phi}} \rangle_{\omega_e=\omega_g,\phi=0}(W)$	$n\ (\mathrm{s^{-1}})$	N	A	$V\ (\mathrm{m^3})$	$P(W)$
(a) 10^{-24}	1	10^3	10^{-33}	4×10^2	10^8
(b) 10^{-25}	10^{-1}	10^2	10^{-34}	4×10	10^7
(c) 10^{-26}	10^{-2}	10	10^{-35}	4	10^6

According to Eqs. (27)–(30) and the above parameters, and setting $\Delta t = 10^3\ \mathrm{s}$, we get the following results (see Table I).

We can see from the results that for scheme (a), although $A = 10^{-33}$, $N = 10^3$, constructing a superconducting toroidal cavity with $V = 4\times 10^2\ \mathrm{m^3}$ will be unrealistic under the present experimental conditions. Nevertheless, in this case the volume of the toroidal cavity is almost two orders of magnitude less than that of the GS scheme, thus a large gap between theoretical schemes and reality would be effectively narrowed. The alternative method is to use strong laser pulse as the background EM wave beam. For example, for the long laser pulse, the instantaneous power of $P = 10^{11}\ \mathrm{W}$ is well within the current technology in short time, less than $10^{-6}\ \mathrm{s}$, but extension to the duration of $10^{-2} - 10^{-1}\ \mathrm{s}$ will be a formidable challenge [6]. For the ultrashort laser pulse, the instantaneous power can reach up to $10^{18} - 10^{21}\ \mathrm{W}$ [19–21], but the duration is limited in $10^{-11}\ \mathrm{s}$ or less. It is unclear yet that whether and how to expand the duration to a longer time. For scheme (c), $A = 10^{-35}$, $n = 10^{-2}\ \mathrm{s^{-1}}$, $N = 10$, $V = 4\ \mathrm{m^3}$, then ratio $n/n^{(0)} \approx 10^{-32}$, this is a very small value, and even under this situation the requirements on some of the relative EM parameters are already limited values of the present experimental possibilities. However, it is remarkable that (1) Because the propagating directions of the tangential perturbed power fluxes are perpendicular to that of the background EM wave, and they have different distributions (unlike usual parametric converters), it provides a new possibility to resolve and display the effect of the GWs at the level of the single photon avalanche effect and in the special

directions inside of the typical laboratory dimensions. (2) Since the effective perturbed power flux and resonance can be concentrated in the region near the axis, the dimensions of the whole systems (including toroidal cavity) can be greatly reduced. For the standing GW of $\lambda_g = 0.1\,\mathrm{m}$, the radius of the focal region can be reduced to the same order of magnitude [see Figs. 1, 7, and Eq. (27)]. The requirements of other parameters can also be further relaxed. (3) For this region near the axis, adopting a ''crystal shield'' to possible leak EM fields from the toroidal cavity has no principle difficulty [some crystals can completely absorb EM waves (photons), but they are transparent to GWs (gravitons)]. (4) The resonant response occurring in the vacuum has neither dielectric dissipation nor the Ohmic losses of the cavity electrodynamical response. Thus the peak values of the perturbed power fluxes can be almost ''instantaneously'' achieved, although it has no energy accumulation effect of the cavity electrodynamical response.

Finally, it should be pointed out that if the power and duration of the background EM wave cannot be further improved upon, and one hopes to increase better the perturbed power fluxes, it would be necessary to raise the strength of the background static magnetic field in the focal region. This is very difficult by the traditional methods. However, it happens that the very strong electrostatic fields can be generated in special regions, called crystal channels [22] where the electrostatic fields can be as large as $10^{12}\,\mathrm{V\,m^{-1}}$, and this is equivalent to a magnetic-field strength of $B \sim 10^4\,\mathrm{T}$. If this effect can be used for such an electrodynamical response, a key breakthrough could be achieved. (Although it is unclear yet how to adopt this effect for the electrodynamical response of the GW's, relative research might become important in the future. For example, see a review on the relative problems in Refs. [22] and [23], including the possibility of an analogy of the relevant phenomena of $10^{-10}\,\mathrm{s}$ after the Big Bang in modern high-energy colliders by the effect.) More research into this subject remains to be done.

ACKNOWLEDGMENTS

This work is supported by the National Nature Science Foundation of China under Grants No. 19575074 and 19835040. The authors gratefully acknowledge Professor V. N. Rudenko and M. V. Sazhin for their helpful discussions and suggestions, and also thank the colleagues of the Sternberg Astronomical Institute of Moscow University for their kind hospitality.

APPENDIX

We present here the concrete expressions of the functions A_1, A_2, B_1, B_2, C_1, and C_2 in solutions (16), which were used in Sec. II:

$$A_1(r,k_e,k_g)=\frac{1}{2}\sum_{p=0}^{\infty}\left(d_{2p}^{+}r^{2p+4}-g_{2p}^{+}r^{2p+2}\right), \tag{A1}$$

$$A_2(r,k_e,k_g)=\frac{1}{2}\sum_{p=0}^{\infty}\left(d_{2p}^{-}r^{2p+4}-g_{2p}^{-}r^{2p+2}\right), \tag{A2}$$

$$B_1(r,k_e,k_g)=\frac{1}{2}\sum_{p=0}^{\infty}\left(d_{2p}^{+}r^{2p+4}+g_{2p}^{+}r^{2p+2}\right), \tag{A3}$$

$$B_2(r,k_e,k_g)=\frac{1}{2}\sum_{p=0}^{\infty}\left(d_{2p}^{-}r^{2p+4}+g_{2p}^{-}r^{2p+2}\right), \tag{A4}$$

$$C_1(r,k_e,k_g)=\sum_{p=0}^{\infty}b_{2p}^{+}r^{2p+3}, C_2(r,k_e,k_g)=\sum_{p=0}^{\infty}b_{2p}^{-}r^{2p+3}, \tag{A5}$$

where

$$\begin{aligned} d_{2p}^{\pm}=(-1)^p Aa\Bigg\{&\frac{1}{[(2p+4)^2-4]}\left(\frac{k_g}{2}\right)^{2p+3}\left[\frac{k_g}{4(p+1)!(p+3)!}\pm\frac{(k_e\pm k_g)}{p!(p+2)!}\right]\\ &+\frac{(k_g^2\pm 2k_ek_g)}{[(2p+4)^2-4][(2p+2)^2-4]}\left(\frac{k_g}{2}\right)^{2p+1}\left[\frac{k_g}{4p!(p+2)!}\pm\frac{(k_e\pm k_g)}{(p-1)!(p+1)!}\right]\\ &+\frac{(k_g^2\pm 2k_ek_g)^2}{[(2p+4)^2-4][(2p+2)^2-4][2p^2-4]}\left(\frac{k_g}{2}\right)^{2p-1}\left[\frac{k_g}{4(p-1)!(p+1)!}\pm\frac{(k_e\pm k_g)}{(p-2)!p!}\right]+\cdots\\ &+\frac{(k_g^2\pm 2k_ek_g)^p}{[(2p+4)^2-4][(2p+2)^2-4]\cdots 60\times 32\times 12}\left(\frac{k_g}{2}\right)^{3}\left[\frac{k_g}{24}\pm\frac{(k_e\pm k_g)}{2}\right]\Bigg\}, \end{aligned} \tag{A6}$$

$$g_{2p}^{\pm}=(-1)^p\frac{Aa}{2}\left\{\frac{1}{(2p+2)^2}\left(\frac{k_g}{2}\right)^{2p}\left[\frac{k_g^2}{4p!(p+2)!}-\frac{(2k_e^2\pm 3k_ek_g+k_g^2)}{(p!)^2}\right]\right.$$
$$+\frac{(k_g^2\pm 2k_ek_g)}{(2p+2)^2(2p)^2}\left(\frac{k_g}{2}\right)^{2p-2}\left[\frac{k_g^2}{4(p-1)!(p+1)!}-\frac{(2k_e^2\pm 3k_ek_g+k_g^2)}{[(p-1)!]^2}\right]$$
$$+\frac{(k_g^2\pm 2k_ek_g)^2}{(2p+2)^2(2p)^2(2p-2)^2}\left(\frac{k_g}{2}\right)^{2p-4}\left[\frac{k_g^2}{4(p-2)!p!}-\frac{(2k_e^2\pm 3k_ek_g+k_g^2)}{[(p-2)!]^2}\right]+\cdots$$
$$\left.+\frac{(k_g^2\pm 2k_ek_g)^p}{(2p+2)^2(2p)^2\cdots 36\times 16\times 4}\left[\frac{k_g^2}{8}-(2k_e^2\pm 3k_ek_g+k_g^2)\right]\right\}, \tag{A7}$$

$$b_{2p}^{\pm}=(-1)^p\frac{Aa}{2}\left\{\frac{\pm 1}{[(2p+3)^2-1]}\left(\frac{k_g}{2}\right)^{2p+2}\left[\frac{k_e}{p!(p+2)!}-\frac{(k_e\pm k_g)}{p!(p+1)!}\right]\right.$$
$$\pm\frac{(k_g^2\pm 2k_ek_g)}{[(2p+3)^2-1][(2p+1)^2-1]}\left(\frac{k_g}{2}\right)^{2p}\left[\frac{k_e}{(p-1)!(p+1)!}-\frac{(k_e\pm k_g)}{(p-1)!p!}\right]$$
$$\pm\frac{(k_g^2\pm 2k_ek_g)^2}{[(2p+3)^2-1][(2p+1)^2-1][(2p-1)^2-1]}\left(\frac{k_g}{2}\right)^{2p-2}\left[\frac{k_e}{(p-2)!p!}-\frac{(k_e\pm k_g)}{(p-2)!(p-1)!}\right]\pm\cdots\cdots$$
$$\left.\pm\frac{(k_g^2\pm 2k_ek_g)^p}{[(2p+3)^2-1][(2p+1)^2-1]\cdots 48\times 24\times 8}\left(\frac{k_g^2}{4}\right)\left[\frac{-k_e}{2}\pm k_g\right]\right\}. \tag{A8}$$

It can be shown that the functions (i.e., the infinite series), $(A_1)-(A_5)$, have an infinite convergence radius and good convergence behavior for r with any finite values.

[1] L. P. Grishchuk and M. V. Sazhin, Zh. Eksp. Teor Fiz. **68**, 1569 (1975) [Sov. Phys. JETP **41**, 787 (1975)].

[2] D. Cuomo *et al.*, *Proceeding of International Symposium on Experimental Gravitational Physics*, Guangzhou, China, 1987, edited by F. C. Michelson (World Scientific, Singapore, 1988), p. 262.

[3] W. K. Logi and A. R. Mickelson, Phys. Rev. D **16**, 2915 (1977).

[4] H. N. Long, D. V. Soa, and T. A. Tuan, Phys. Lett. A **186**, 382 (1994).

[5] G. Gratta, K. J. Kim, A. Melissions, and T. Tauchi, *Workshop on Beam-Beam and Beam-Radiation Interaction: High Intensity and Nonlinear Effects*, Los Angeles, California, 1991, edited by C. Pellegrini *et al.* (World Scientific, Singapore, 1992), p. 70.

[6] P. Chen, G. D. Palazzi, K. J. Kim, and C. Pellegeini (Ref. [5]), p. 84.

[7] P. Fortini, C. Gualdi, and A. Ortolan, Nuovo Cimento Soc. Ital. Fis., B **106**, 395 (1991).

[8] D. Boccaletti, V. D. Sabbata, and P. Fortini, Nuovo Cimento Soc. Ital. Fis., B **70**, 129 (1970).

[9] L. P. Grishchuk and M. V. Sazhin, Zh. Eksp. Teor. Fiz. **84**, 1937 (1983) [Sov. Phys. JETP **53**, 1128 (1983)].

[10] M. X. Tang, F. Y. Li, and J. Luo, Acta Phys. Sin. **6**, 161 (1997).

[11] F. Y. Li and M. X. Tang, Chin. Phys. Lett. **16**, 12 (1999).

[12] U. H. Gerlach, Phys. Rev. D **46**, 1239 (1992).

[13] V. Faraoni, Nuovo Cimento Soc. Ital. Fis., B **107**, 631 (1992).

[14] A. Yariv, *Quantum Electronics*, 2nd ed. (Wiley, New York, 1975).

[15] G. Boebinger, A. Passner, and J. Bevk, Sci. Am. (Int. Ed.) **272**, 34 (1995).

[16] I. M. Pinto and G. Rotoli, *In the 8th Italian Conference on General Relativity and Gravitational Physics*, edited by M. G. Gerdoonio *et al.* (World Scientific, Singapore, 1989), p. 560.

[17] V. B. Braginsky, *System with Low Dissipation* (Nauka, Moscow, 1981).

[18] J. D. Jakson, *Classical Electrodynamics* (Wiley, New York, 1975).

[19] J. C. Kieffer, Phys. Fluids B **5**, 2676 (1993).

[20] M. Tabak *et al.*, Phys. Plasmas **1**, 1626 (1994).

[21] A. Modena *et al.*, Nature (London) **377**, 606 (1995).

[22] P. Chen, *Resonant Photon-Graviton Conversion in EM Fields: From Earth to Heaven*, Stanford Linear Accelerator Center-PUB-6666 (September, 1994).

[23] P. Chen and R. J. Noble, *Crystal Channel Collider; Ultra-High Energy and Luminosity in the Next Century*, Stanford Linear Accelarator Center-PUB-7402 and Fermilab-Conf 96/441 (January, 1997).